Journal of Porous Materials 12: 183–191, 2005

Nitrous Oxide Reduction with Ammonia and Methane Over Mesoporous Silica Materials Modified with Transition Metal Oxides

L. CHMIELARZ*, P. KUŚTROWSKI, M. KRUSZEC AND R. DZIEMBAJ
Jagiellonian University, Faculty of Chemistry, Ingardena 3, 30-060 Krakow, Poland
chmielar@chemia.uj.edu.pl

P. COOL AND E.F. VANSANT
Department of Chemistry, University of Antwerp, Laboratory of Inorganic Chemistry, Universiteitsplein 1, 2610 Wilrijk, Belgium

Received October 29, 2004; Revised March 4, 2005

Abstract. Transition metal oxides (Cu, Cr and Fe) were deposited on various mesoporous silicas (MCM-48, SBA-15, MCF and x-MSU) by an impregnation method. Electron microprobe analysis, BET, UV-VIS-DRS and temperature programmed desorption of NH_3 were used for the characterization of the samples. The modified mesoporous silicas were tested as catalysts of the N_2O decomposition and the N_2O reduction using ammonia and methane. The Cu-containing samples presented the highest catalytic activity in the N_2O decomposition, while the Cr- and Fe-modified materials were more active in the reduction of nitrous oxide with NH_3 and CH_4. The type of the silica support strongly influenced the catalytic performance of the studied materials.

Keywords: mesoporous silicas, transition metals, catalysis, N_2O decomposition, N_2O reduction, ammonia, methane

1. Introduction

Nitrous oxide contributes to the destruction of ozone layer in the stratosphere and is considered as a strong greenhouse gas. The concentration of N_2O in the atmosphere increases by about 0.2–0.3% per year and is caused mainly by anthropogenic activities [1, 2]. The major source of the nitrous oxide emission is the chemical industry (e.g. production of nitric acid, adypic acid, caprolactam, glyoxal) [3]. The most promising way for the reduction of the N_2O emission is its catalytic decomposition to nitrogen and oxygen. However, the studied catalysts of this process effectively operate in a relatively high temperature range and are therefore not acceptable for the industrial applications. The nitrous oxide decomposition proceeds according to a redox mechanism [4]. N_2O molecules oxidise active centres, which have to be reduced in order to start the next catalytic cycle. The reduction of active sites is a rate determining step of this process. It seems to be possible to increase the rate of the N_2O decomposition by using an additional reagent, which can remove oxygen bonded to the active sites. Hydrocarbons [5, 6] and ammonia [7, 8] are main candidates that can be used as reducing agents in this process.

Mesoporous silicas, which are characterised by a very high surface area, ordered porous structure and high thermal stability, are very promising supports for catalytic applications. The modification of these silica materials with transition metal oxides results in the formation of the redox centres. It is possible to obtain different loading and dispersion of transition metal oxides by using various deposition methods (e.g. impregnation or grafting) [9–12]. This paper presents the study

---

*To whom correspondence should be addressed.

of mesoporous silica materials modified with selected transition metal oxides (Cu, Cr, Fe) as catalysts for the processes of nitrous oxide conversion.

2. Experimental

2.1. Catalysts Preparation

Four different mesoporous silicas (MCM-48, SBA-15, MCF, x-MSU) were used as supports for deposition of transition metal (Cu, Cr, Fe) oxides.

For synthesis of MCM-48, $C_{16\text{-}12\text{-}16}$ Gemini and NaOH were dissolved in distilled water [13]. Then, fumed silica (Aerosil 380) was added under vigorous stirring. The mixture was stirred at room temperature for 30 min and then the resulting gel was transferred into an autoclave and aged at 130°C for 3 days. Subsequently, it was filtered, washed with distilled water, resuspended in distilled water, transferred into autoclave and aged for 24 h at 130°C. This procedure was repeated twice. The final product was separated by filtration, washed with distilled water and dried at room temperature.

Mesoporous silica SBA-15 was synthesized according to the procedure described earlier by Van Bavel et al. [14]. Poly(ethylene oxide)-*block*-poly(propylene oxide)-*block*-poly(ethylene oxide) triblock copolymer ($EO_{20}PO_{70}EO_{20}$, Pluronic P123) was dissolved in 1.6 M HCl and then suitable amount of tetraethyl orthosilicate (TEOS) was added. The obtained suspension was stirred at 45°C for 8 h and then aged at 80°C for 15 h. The solid product was filtered, washed with distilled water and dried at room temperature.

The synthesis MCF was performed according to the procedure described by Schmidt-Winkel et al. [15]. Pluronic P123 was dissolved in aqueous HCl solution (1.6 M). Then, NH_4F and 1,3,5-trimethylbenzene were added and vigorous stirred for 1 h. Subsequently, tetraethyl orthosilicate (TEOS) was added to the reaction mixture. After 20 h, the slurry was transferred to an autoclave and aged at 100°C for 24 h. The obtained precipitate was filtered, washed with distilled water, and dried in air.

The synthesis of MSU was performed using a modified procedure described by Kim et al. [16]. Sodium silicate was dissolved in distilled water and mixed with surfactant (brij 56) and acetic acid. After 1 h, NaF was added and the resulting gel was left at 60°C for 3 days under vigorous stirring. Finally, the product was filtered, washed with distilled water and dried at room temperature.

Transition metal (Cu, Cr, Fe) oxides were deposited on the mesoporous silica materials by an incipient wetness impregnation using aqueous solutions of $Cu(NO_3)_2{\cdot}3H_2O$, $Cr(NO_3)_3{\cdot}9H_2O$ or $Fe(NO_3)_3{\cdot}9H_2O$. The amount of metal nitrates used was calculated to obtain 3 wt% of transition metal in the calcined catalyst. The samples were dried at room temperature for 3 days and then calcined in static air at 450°C for 3 hours.

2.2. Catalyst Characterisation

The concentration of transition metal oxide deposited on the support was determined by electron microprobe analysis (JEOL Superprobe 733).

Porosity and surface area studies were performed on a Micromeritics ASAP 2010 automated gas adsorption system. All the samples were outgassed at 350°C under vacuum prior to N_2 adsorption at -196°C. Surface areas were calculated according to the BET equation, while pore size distributions were derived from the adsorption isotherm using the BJH model.

The UV-VIS-DRS spectra of calcined materials were recorded on a Nicolet Evolution 500 spectrophotometer. The measurements have been performed in the range of 200–800 nm for samples diluted in KBr (2 wt%).

The surface concentration of acidic centres was determined by temperature-programmed desorption of ammonia (NH_3-TPD). Experiments were carried out in the range of 70–600°C in a fix-bed flow microreactor (i.d., 4.5 mm; l., 240 mm). The temperature in the catalyst bed was measured by a K-type thermocouple located in a quartz capillary immersed in the catalyst bed. The molecules desorbing from sample were monitored on-line by a quadrupole mass spectrometer (VG QUARTZ). Prior to the NH_3-TPD experiments, a catalyst (50 mg) was outgassed at 550°C for 1 h in a flow of dry helium (20 ml/min). Subsequently, sample was cooled down to 70°C and saturated for about 30 min in a flow of 1% NH_3/He mixture (20 ml/min). Then, sample was purged in a helium flow until a constant baseline level was attained. Desorption was carried out with a linear heating rate (10°C/min) in a flow of He (20 ml/min). The NH_3-TPD spectra were obtained from the $m/z = 16$ mass-to-charge signal ratio after a calibration procedure with a commercial NH_3/He mixture.

2.3. Catalytic Measurements

Catalytic measurements have been performed in a fixed-bed flow reactor (i.d., 7 mm; l., 240 mm). Prior to the activity test, each sample was outgassed in pure helium at 550°C for 1 h. Then, the sample was cooled to 100°C and a flow of pure helium was switch for a reaction mixture. The measurements of the catalytic activity were performed in intervals of about 50°C. The reactor was kept at a given temperature at least for 30 minutes after the reaction had reached a steady-state. The following compositions of the reacting mixtures were used in the catalytic tests:

(a) *N_2O decomposition* – 0.5 vol.% of N_2O in helium, total flow rate — 40 ml/min;
(b) *N_2O reduction by NH_3* – 0.5 vol.% of N_2O and 0.5 vol.% of NH_3 in helium, total flow rate — 40 ml/min;
(c) *N_2O reduction by CH_4* – 0.5 vol.% of N_2O and 0.5 vol.% of CH_4 in helium, total flow rate — 40 ml/min.

Quadrupole mass spectrometer (VG QUARTZ) was used for analysis of outlet gases in the case of the N_2O decomposition (a) and N_2O reduction with ammonia (b). Gaseous products in the nitrous oxide reduction by methane (c) were analyzed by a gas chromatograph (Varian 3400 CX) equipped with two packed columns (molecular sieves 5A and Porapak Q) as well as TCD and FID detectors.

3. Results and Discussion

The transition metal content determined by electron microprobe analysis as well as the textural parameters of the mesoporous silica materials are comparatively presented in Table 1. The MCM-48 sample is characterised by a very high surface area (1115 m^2/g) and a large pore volume (1.047 cm^3/g). These parameters were significantly reduced after the deposition of transition metal oxides. This effect is the most pronounced for the Cu-MCM-48 sample, which exhibited a decrease in the surface area and total pore volume by about 10 and 14%, respectively. The modification of MCM-48 with chromium and iron also caused a decrease in the textural parameters, however the changes in the surface area and pore volume are significantly lower and equal to about 5.5–5.8% and 7.4–8.6%, respectively. It should be noticed that the modification of MCM-48 with copper resulted in a decrease in the maximum of pore diameter from 30 to 27 Å. Such effect was not observed for the Cr and Fe-modified samples. Transition metals oxides deposited on SBA-15 decreased also the textural parameters of the parent material. Copper oxide introduced to the SBA-15 support reduced its surface area and pore volume by about 14 and 11%, respectively. Similar effects were observed for Cr and Fe-modified SBA-15, however the changes of textural parameters are not so important. The MCF material is characterised by a very large pore diameter, which exceeds 300 Å, and a high pore volume. The deposition of transition metal oxides on the MCF support resulted in a decrease in the maximum of pore diameter, surface area and pore volume. Similarly to the SBA-15 and MCM-48 samples, the deposition of copper resulted in a significant decrease in textural parameters of MCF. Introduction of transition metal oxides onto the MSU support reduced the surface area and pore volume by about 8–10% and 2.5–3.1%, respectively. The maximum of pore diameter decreased from 153 to 130 Å after the deposition of transition metal oxides.

Table 1. Transition metal content and textural parameters of modified mesoporous catalysts.

Sample	Transition metal content (wt.%)	Max BJH pore diameter (Å)	S_{BET} (m^2/g)	V_{total} (cm^3/g)
MCM-48	–	30	1115	1.047
Cu-MCM-48	2.8	27	1007	0.897
Fe-MCM-48	3.8	30	1050	0.969
Cr-MCM-48	4.0	30	1054	0.957
SBA-15	–	56	580	0.611
Cu-SBA-15	3.8	56	499	0.544
Fe-SBA-15	2.7	56	535	0.552
Cr-SBA-15	3.1	56	518	0.547
MCF	–	308	638	2.272
Cu-MCF	4.1	233	527	1.424
Fe-MCF	2.5	234	566	1.640
Cr-MCF	2.4	260	549	1.708
MSU	–	153	206	0.612
Cu-MSU	5.3	130	185	0.596
Fe-MSU	5.4	130	189	0.597
Cr-MSU	4.5	130	190	0.593

The results of the catalytic experiments are comparatively presented in Fig. 1. The Cu-containing samples have been found to be significantly more active for the N_2O decomposition compared to their chromium or iron analogues. However, it must be pointed out

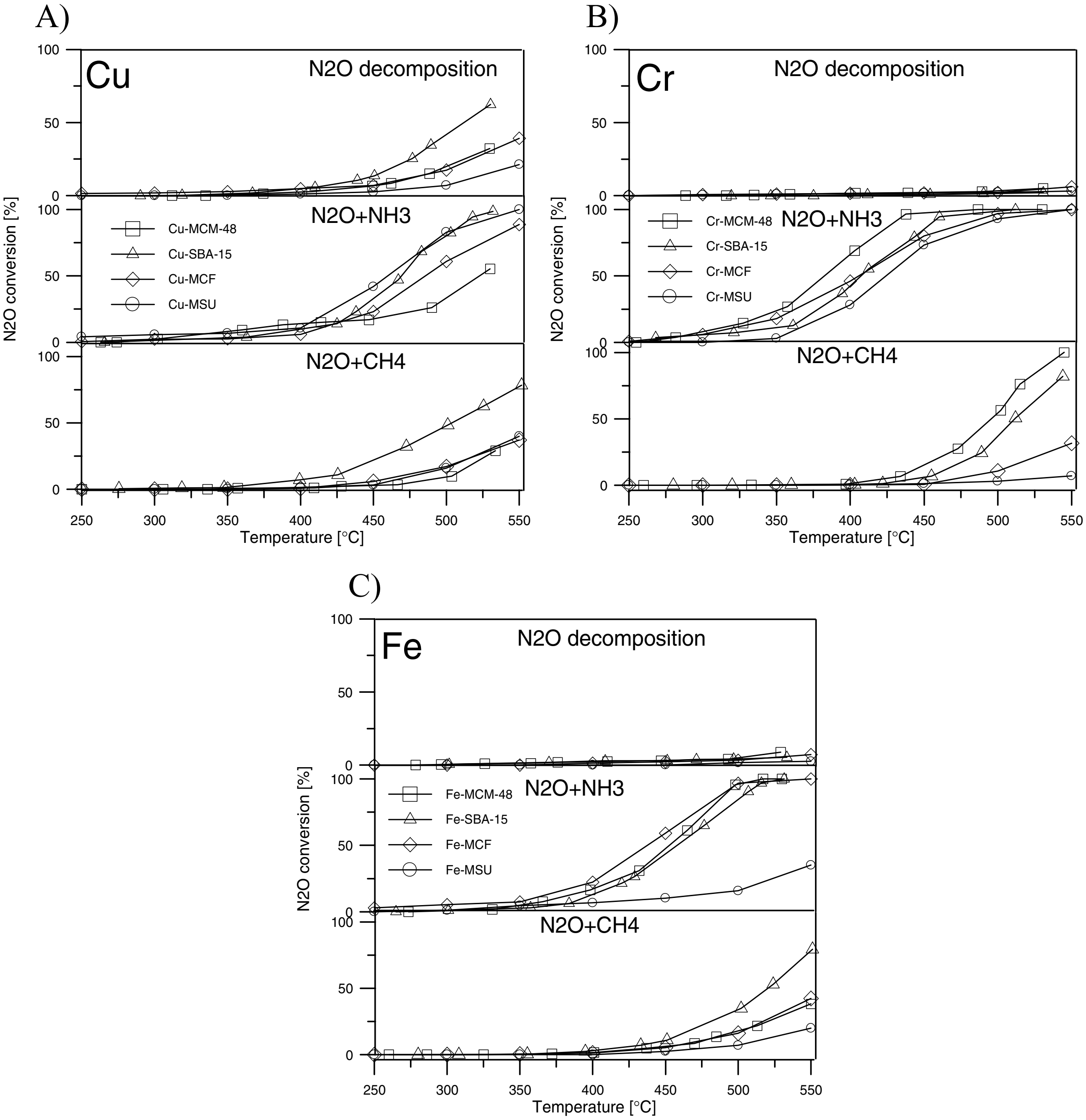

Figure 1. Catalytic decomposition and reduction of N_2O by ammonia and methane over the Cu (A), Cr (B) and Fe-modified (C) mesoporous silicas.

that the reaction over the Cu-modified silicas started at rather high temperature (about 360°C) and 100% of N_2O conversion was not reached up to 550°C (Fig. 1(A)). Furthermore, the highest rate of the N_2O decomposition was measured for the Cu-SBA-15 catalyst. The catalysts based on the MCM-48 and MCF supports were less active, while the lowest activity was found for the Cu-MSU sample. Decomposition of N_2O was not detected over the mesoporous silicas modified with chromium (Fig. 1(B)) or iron oxides (Fig. 1(C)) up to 450°C. The N_2O conversion slowly increased above this temperature, however, did not exceeded 10% in the whole studied temperature range.

The reaction mechanism [4, 8] proposed for the decomposition of N_2O over the catalysts containing transition metal oxides consists of the following steps:

$$N_2O + {}^* \rightarrow N_2O^* \tag{1}$$

$$N_2O^* \rightarrow N_2 + O^* \tag{2}$$

$$2O^* \rightarrow O_2 + 2^* \tag{3}$$

or/and

$$O^* + N_2O \rightarrow N_2 + O_2 \tag{4}$$

The reactions (3) and (4) are supposed to be the rate determining steps. It should be therefore assumed that the redox properties of transition metal oxide influence strongly its catalytic activity in this process. It was shown [17] that the thermal reduction of CuO occurred even in air atmosphere at elevated temperatures. CuO appeared to be easier reducible compared to iron and chromium oxides. Thus, higher catalytic activity of the Cu-containing catalysts is probably related to specific redox properties of copper oxide. In order to increase the rate of the active sites (O*) reduction reducing agents (CH_4, NH_3) were added into the reaction mixture.

A significant increase in the N_2O conversion was observed after an addition of ammonia into the reactant stream. Nitrogen and water vapor were the only detected reaction products. The chromium oxide doped silicas, which were inactive in the N_2O decomposition process, have catalyzed the nitrous oxide conversion more effectively than the Cu and Fe-containing materials. Furthermore, the type of mesoporous silica, used as support material for the chromium deposition strongly influenced the catalytic activity. The nitrous oxide conversion obtained for the Cr-MCM-48 sample (Fig. 1(B)), which was considerably more active in the N_2O conversion by ammonia than the other Cr-modified silicas, started at a temperature as low as 250°C and reached 100% of N_2O conversion at about 450°C. The Cr-SBA-15 catalyst was less active and 100% of nitrous oxide conversion was obtained at about 500°C. The reaction rates for the Cr-MCF and Cr-MSU catalysts were significantly lower and 100% of N_2O conversion was obtained at temperature above 500°C. The N_2O conversion by ammonia over the Fe-containing silicas started at about 300°C and reached 100% at temperature above 500°C (with exception of Fe-MSU). The highest activity in a series of the Fe-modified silicas was measured for the Fe-MCF catalyst, however only slightly less activity was found for Fe-MCM-48 and Fe-SBA-15. Surprisingly low N_2O conversion, which did not exceed 40% at 550°C, was measured for the Fe-MSU catalyst. Ammonia introduced into the reaction stream only slightly increased the N_2O conversion measured over the Cu-modified silicas. The Cu-SBA-15 and Cu-MSU samples have been found to be more active than Cu-MCF, while the Cu-MCM-48 catalyst presented the lowest activity.

Methane was a significantly less effective reducer of N_2O than ammonia. Only small differences in the N_2O conversion were observed for the reactions performed over the Cu-modified silicas in the presence and absence of methane (Fig. 1(A)). The highest activity in a series of the Cu-modified samples has been measured for the Cu-SBA-15 catalyst. The other Cu-doped materials were significantly less active. The N_2O conversion by methane over the Cr-modified samples started at temperature about 400°C. The type of mesoporous support used for the deposition of chromium oxide strongly influenced the catalytic activity for this process. The highest increase in the nitrous oxide conversion was observed over the Cr-MCM-48 catalyst. Lower catalytic activity was measured for Cr-SBA-15, while the catalysts based on the MCF and MSU silicas presented the lowest activity.

The obtained results show that ammonia reduces N_2O much more effectively than methane. The type of transition metal oxide deposited on the support is a crucial factor influencing the catalytic performance of the studied materials. The activity of transition metal oxides for the reduction of N_2O by ammonia can be presented in the following sequence: Cr > Fe > Cu. The type of mesoporous silica, used as a carrier, also influences the activity, however, this factor is not as important as deposited transition metal oxide.

Addition of reducing agents (CH_4, NH_3) into the reaction mixture significantly increased the N_2O conversion over the Cr- and Fe-containing catalysts. This effect was significantly less distinct for the Cu modified samples. Thus, it seems that ammonia and methane effectively reduced oxidized active sites (O*) and therefore increased the rate of the N_2O conversion.

The coordination of the transition metal oxide species present on the catalyst surfaces was studied by the UV-VIS-DRS method. The original spectra recorded for the Cu-modified samples were fitted by four bands (Fig. 2(A)). The first maximum (200–230 nm) is related to the presence of surface Cu^+ species [18]. The band centred at about 270–

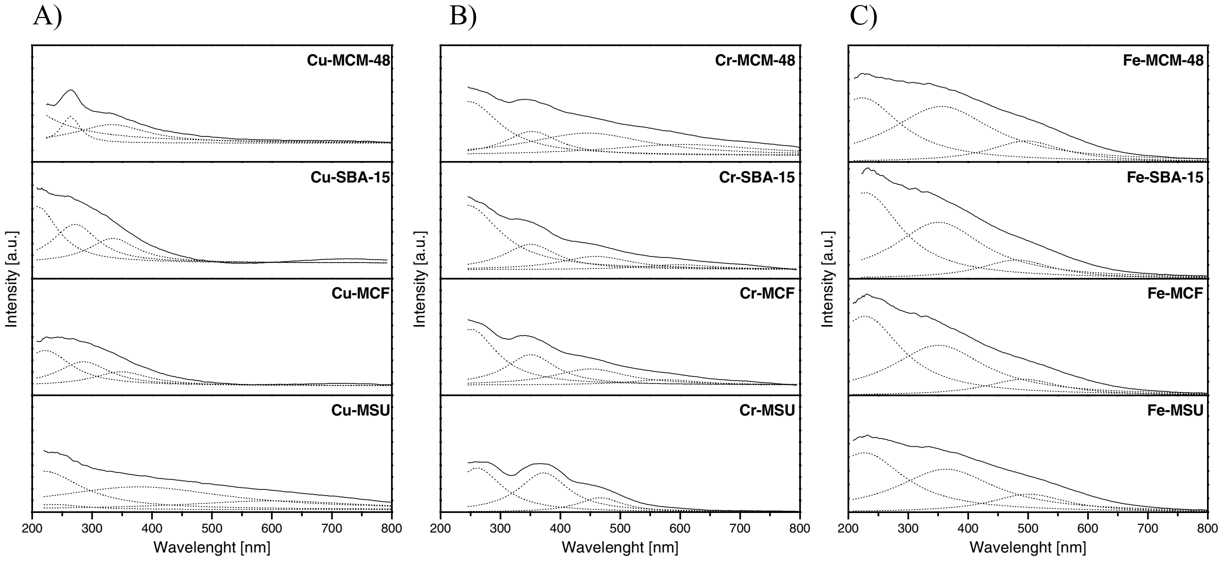

Figure 2. UV-VIS-DRS spectra obtained for the mesoporous silicas modified with copper (A), chromium (B) and iron (C).

280 nm can be attributed to the charge-transfer between mononuclear Cu^{2+} and oxygen, whereas the maximum at around 340-380 nm is caused by the presence of $[Cu\text{-}O\text{-}Cu]_n$-type surface clusters [19–21]. Moreover, the band at about 600 nm can be attributed to the d-d transition of Cu with an octahedral environment in CuO [22, 23]. The obtained results show that copper is present on the catalyst surface in the form of various species. However, different distribution of these species has been found for the Cu-modified materials. It seems that copper is much better dispersed on the surface of SBA-15 than on the other supports. On contrary, copper deposited on MSU is probably present mainly in the form of CuO crystallites. These results are supported by observed colours of the Cu-containing samples. The Cu-MSU sample is grey, while the other catalysts are brightly green in colour.

For the sample Cr-MSU, three bands have been detected (Fig. 2(B)). The bands at 260–280 and 330–350 can be attributed to the presence of Cr^{6+} [24]. Because chromium(III) nitrate was used during the deposition, an oxidation of chromium must be assumed during the calcination in air. The band at 470 nm is related to the presence of chromate or dichromate species being in the contact with the support surface [25]. For the Cr-MCM-48, Cr-SBA-15 and Cr-MCF samples besides, the presence of Cr^{6+} also bands related to Cr^{3+} were detected. The maxima at 450–460 and 580–600 nm can be attributed to $A_{2g} \rightarrow T_{1g}$ and $A_{2g} \rightarrow T_{2g}$ charge transfers typical of octahedrally coordinated Cr^{3+}. The colours of the Cr-containing samples are different. The Cr-MCM-48 catalyst is orange, while the other Cr-modified samples are yellow in colour. These differences in the samples colour can be related to larger concentration of chromium species on the outer surface of MCM-48 or by presence of chromium mainly in the form of dichromates.

Three bands were obtained for all the Fe-modified materials (Fig. 2(C)). The band, with a maximum at about 240 nm is related to the isolated Fe^{3+} cations, while the second one, centred at about 360 nm corresponds to small oligonuclear $(FeO)_n$ species [12, 26, 27]. The broad band in the range 350–550 nm can be assigned to symmetrical and spin forbidden d-d transitions of Fe^{3+} [28]. The samples slightly differ in colours. Fe-SBA-15 is brightly yellow, the Fe-MCF and Fe-MSU catalysts are yellow, while Fe-MCM-48 is brightly brown. These differences in colour are probably caused by different concentrations of Fe-species deposited on the outer surface of the supports. Probably, the Fe-MCM-48 sample contains more Fe-species on the outer surface of the support in comparison to the other samples. It should be noticed that among the studied silica supports MCM-48 is characterized by the smallest pore diameters. Therefore, deposition of significant amount of active phase on the outer surface of the MCM-48 support could be predicted.

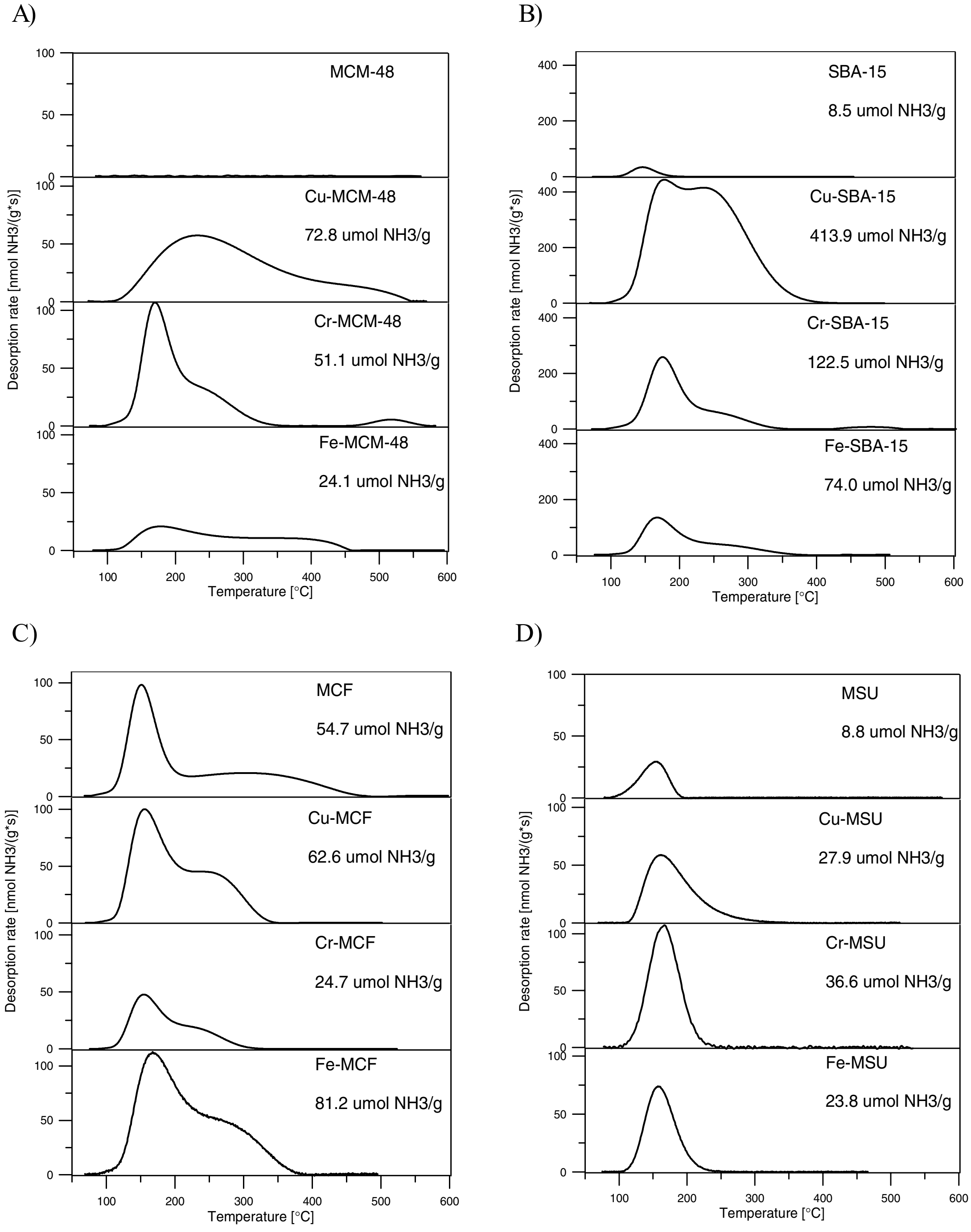

Figure 3. NH_3-TPD patterns obtained for the MCM-48 (A) SBA-15 (B), MCF (C) and MSU (D) samples.

The next factor that could influence activity of the catalysts, especially in the case of the N_2O reduction by ammonia, is the surface acidity of samples. The concentration and the strength of the surface acid sites were determined by the temperature-programmed desorption of ammonia (NH_3-TPD). Results of these studies are presented in Fig. 3. The pure mesoporous silicas have shown different surface acidities. In the case of MCM-48, desorption of NH_3 was not detected. Only a very small ammonia desorption maximum was found for the SBA-15 and MSU supports. Significantly higher amount of chemisorbed ammonia was measured for MCF. The desorption spectrum measured for MCF consists of two unresolved maxima centered at 160 and 320°C. These differences in the surface acidity of the supports could be related to the conditions of their synthesis. MCM-48, for which any acidity was not detected, was synthesized under basic conditions. While the other carriers were prepared in an acidic medium. Modification of MCM-48 with transition metal oxides resulted in an increase of the ammonia chemisorption (Fig. 3(A)). The NH_3-TPD pattern recorded for the Cu-MCM-48 sample is spread in the temperature range of 120–540°C and consists of two unresolved maxima centered at about 230 and 450°C. Weakly chemisorbed NH_3 molecules desorb from the surface of Cr-MCM-48 in the two stages. The first sharp maximum is centered at 190°C, while the second one, much broader, at about 250°C. A small and broad desorption peak indicating the presence of strongly bounded ammonia has been detected at significantly higher temperatures (460–570°C). The surface concentration of chemisorbed ammonia on the Fe-MCM-48 sample is considerably lower than for the Fe or Cr-modified supports. The desorption pattern is spread in the range of 110–460°C and consists of at least two unresolved maxima centered at 170 and 370°C. The modification of SBA-15 with transition metal oxides resulted in a significant increase in ammonia chemisorption (Fig. 3(B)). The highest amount of chemisorbed ammonia, in this series of samples, was detected for Cu-SBA-15. The desorption pattern consists of two very intensive peaks centered at 180 and 250°C. Desorption maxima for Cr-SBA-15 and Fe-SBA-15 were measured at very similar temperatures, however the intensity of these peaks, especially the high-temperature one, are much lower than in the case of the Cu-containing sample. The high temperature maximum (420–520°C), related to a small amount of strongly chemisorbed ammonia, was detected for Cr-SBA-15. The shapes of the desorption curves obtained for MCF (Fig. 3(C)) modified with transition metal oxides are very similar to those recorded for SBA-15 doped with Cr or Fe. However, the intensity of desorption peaks is lower in the case of the Cu-MCF and Cr-MCF samples. For Fe-SBA-15 and Fe-MCF, not only the shape of desorption pattern but also the intensity of the peaks are nearly the same. It should be noticed that the modification of MCF with transition metal oxides resulted in a disappearance of ammonia desorption at temperature above 390°C. Probably, the deposition of transition metal oxides on the MCF surface resulted in a removal or modification of the strong acid centers. Only weakly chemisorbed ammonia, which desorbs in the low temperature region (Fig. 3(D)), was detected for the MSU samples. The modification of MSU with transition metal oxides resulted in an increase in the surface concentration of chemisorbed ammonia, however the measured quantity of desorbing NH_3 is very low.

Transition metal oxides deposited on the surface of the support influence the concentration and thermal stability of chemisorbed ammonia. This effect could be explained by the formation of donor-acceptor bonds between free electron pair of ammonia molecule and unoccupied d orbital of transition metals [29]. It is difficult to find a simple correlation between surface concentration of chemisorbed ammonia and the catalytic performance of the studied catalysts. However, a series of MSU samples, which have been found to be the least active catalysts in the reaction using ammonia (with the exception of the Cu-MSU) were characterized by the presence of only weakly chemisorbed ammonia. Therefore, for these catalysts chemisorbed ammonia molecules can not be present on the catalyst surface under the reaction conditions used. The other mesoporous silicas are characterized by stronger chemisorbed ammonia. Therefore, chemisorbed ammonia can be involved in the reaction with N_2O. In the case of Cr-MCM-48 and Cr-SBA-15, which have been found to be the most active catalysts, strongly chemisorbed ammonia, which desorbs in the temperature range of 430–570°C, could play an important role in the nitrous oxide conversion.

4. Conclusions

Mesoporous silicas modified with transition metals were studied as catalysts of the N_2O decomposition and the reduction of nitrous oxides by ammonia and methane. The Cu-containing samples have been found to be the most active catalysts for the N_2O decomposition. The type of the support used to copper deposition strongly influenced the catalytic performance. Among the copper doped silicas, Cu-SBA-15 was significantly more active catalyst in the N_2O decomposition than Cu-MCM-48 and Cu-MCF, while the lowest activity was measured for the Cu-MSU catalyst. The Cr- and

Fe-modified silicas have shown a poor activity in the N_2O decomposition.

Introduction of ammonia or methane into the reaction mixture considerably increased the N_2O conversions over the Cr- and Fe-containing catalysts. NH_3 was found to be significantly more effective reducer of nitrous oxide than CH_4. The highest catalytic activity in the N_2O reduction by ammonia was measured for the Cr-MCM-48 samples. The other Cr-modified samples were less active. Lower activity was measured also for the Fe-containing catalysts, which totally converted N_2O at temperatures above 475°C (with exception of Fe-MSU). The type of support as well as deposited transition metal oxide strongly influenced activity of the catalysts in the reduction of N_2O with methane. Among the Cu- and Fe-containing silicas, the SBA-15 based catalysts were the most active, while in a series of the Cr-modified materials, the Cr-MCM-48 catalyst presented the highest activity.

The impregnation method, which was used for the deposition of transition metals on the supports, resulted in the formation of different species on the support surface. The mononuclear Cu^+ and Cu^{2+} species as well as $[Cu\text{-}O\text{-}Cu]_n$ surface clusters and CuO were identify in the case of the Cu-containing catalysts. For the chromium modified samples the surface species containing Cr^{6+} and Cr^{3+} were detected, while isolated Fe^{3+} and clustered $(FeO)_n$ species were found for the Fe-modified silicas.

The surface acidity of the catalysts depended on both the type of mesoporous silicas used as support and introduced transition metal oxide. There was not found a simple correlation between the surface acidity and the catalytic performance of the studied samples. However, it seems that the presence of strong acidic centers is an important factor affecting the activity of the catalysts in the N_2O conversion by ammonia.

Acknowledgment

The authors thank the Ministry of Flanders and the Polish Ministry of Scientific Research and Information Technology for financial support in the frame of bilateral Flemish-Polish project for 2004–2005.

References

1. R.F. Weiss, J. Geophys. Res. **86**, 7185 (1981).
2. M.A.K. Khalil and R.A. Rasmussen, Tellus B **35**, 161 (1983).
3. G.M. Marnellos, E.A. Efthimiadis, and I.A. Vasalos, Appl. Catal. B. **46**, 523 (2003).
4. F. Kapteijn, J. Rodriguez-Mirasol, and J.A. Moulijn, Appl. Catal. B **9**, 25 (1996).
5. C. Pophal, T. Yogo, K. Tanabe, and K. Segawa, Catal. Lett. **44**, 271 (1997).
6. K. Yamada, C. Pophal, and K. Segawa, Micropor. Mesopor. Mater. **21**, 549 (1998).
7. M. Mauvezian, G. Delahay, B. Coq, and S. Kieger, Appl. Catal. B. **23**, L79 (1999).
8. K. Aika, M. Isobe, K. Kido, T. Moriyama, and T. Onishi, J. Chem.Soc., Faraday Trans. 1 **83**, 3139 (1987).
9. I.V. Babich, Y.V. Plyuto, P. Van Der Voort, and E.F. Vansant, J. Coll. Interface Sci. **189**, 144 (1997).
10. M. Baltes, O. Collart, P. Van Der Voort, and E.F. Vansant, Langmuir **15**, 5841 (1999).
11. D. Zhao, C. Nie, Y. Zhou, S. Xia, L. Huang, and Q. Li, Catal. Today **68**, 11 (2001).
12. M.V. Landau, E. Dafa, M.L. Kaliya, T. Sen, and M. Hereskowitz, Micropor. Mesopor. Mater. **49**, 65 (2001).
13. O. Collart, P. Van Der Voort, E.F. Vansant, D. Displantier, A. Galazneau, P. Di Renzo, and F. Fajula, J. Phys. Chem. B **105**, 12771 (2001).
14. E. Van Bavel, P. Cool, K. Aerts, and E.F. Vansant, J. Phys. Chem. B **108**, 5263 (2004).
15. P. Schmidt-Winkel, W.W. Lukens, D. Zhao, P. Yang, B.F. Chmelka, and G.D. Stucky, J. Am. Chem. Soc. **121**, 254 (1991).
16. S.S. Kim, A. Karkamkar, T.J. Pinnavaia, M. Kruk, and M. Jaroniec, Phys. Chem **105**, 7663 (2001).
17. L. Chmielarz, P. Kustrowski, D. Majda, A. Rafalska-Łasocha, and R. Dziembaj, Appl. Catal B **35**, 195 (2002).
18. M.C.N.A. De Carvalho, F. B. Passo, and M. Schmal, Appl. Catal. A **193**, 265 (2000).
19. F.M.T. Mendes and M. Schmal, Appl. Catal. A **151**, 393 (1997).
20. M. Ramakrishna Prasad, G. Kamalakar, S.J. Kulkarni, and K.V. Raghavan, J. Mol. Catal. A **180**, 109 (2002).
21. S. Velu, K. Suzuki, M. Okazaki, M.P. Kapoor, T. Osaki, and F. Ohashi, J. Catal. **194**, 373 (2000).
22. M. Shimokawabe, H. Asakawa, and N. Takezawa, Appl. Catal. **59**, 45 (1990).
23. G. Centi, S. Perathoner, D. Biglino, and E. Giamello, J. Catal. **151**, 75 (1995).
24. G. Neri, A. Pistone, S. De Rossi, E. Rombic, C. Milone, and S. Galvagno, Appl. Catal. A **260**, 75 (2004).
25. A.B. Gaspar, J.L.F. Brito, and L.C. Dieguez, J. Mol. Catal. A **203**, 251 (2003).
26. M.A. Wojtowicz, J.R. Pels, and J.A. Moulijn, Fuel Proc. Technol. **34**, 1 (1993).
27. R.A. Reimer, S.C. Slaten, M. Seapan, M.W. Lower, and P.E. Tomlinson, Environ. Progr. **13**, 134 (1994).
28. E. Suzuki, K. Nakashiro, and Y. Ono, Chem. Lett. 953 (1988).
29. G. Busca, L. Letti, G. Ramis, and F. Berti, Appl. Catal. B **18**, 1 (1998).